Rising methane emissions from Finnish lakes due to climate warming and increasing ice-free days

Mingyang Guo[1], Qianlai Zhuang[1], Zeli Tan[2], Narasinha J.f Shurpali[3], Sari Juutinen[4], Pirkko Kortelainen[5], and Pertti J Martikainen[3]

[1]Purdue University
[2]Pacific Northwest National Laboratory (DOE)
[3]University of Eastern Finland
[4]University oh Helsinki
[5]Finnish Environment Institute

November 22, 2022

Posted on 22 Nov 2022 — CC-BY-NC-ND 4 — https://doi.org/10.1002/essoar.10501637.1 — This a preprint and has not been peer reviewed. Data may be preliminary.

Abstract

Lakes account for about 10% of the boreal landscape and are responsible for approximately 30% of biogenic methane emissions. However, its quantification is still of large uncertainty under changing climate conditions. Finland has the densest lake system in the world with most lakes situated in the boreal zone. This study uses a large observational dataset of lake methane concentrations to constrain its methane emissions with an extant process-based lake biogeochemical model. We found that the total current diffusive emission from Finnish lakes is 0.12±0.03 Tg CH yr and will increase by 26-59% by the end of this century. We discovered that while warming lake water and sediment temperature played an important role, the climate impact on ice-on periods was a key indicator to the degree of emission increase in the future. We concluded that these boreal lakes remain as a significant methane source under warming climate in this century.

[Geophysical Research Letter]

Supporting Information for

[Rising methane emissions from Finnish lakes due to climate warming and increasing ice-free days]

Mingyang Guo[1], Qianlai Zhuang[1,2], Zeli Tan[3], Narasinha Shurpali[4], Sari Juutinen[5], Pirkko Kortelainen[6], Pertti J. Martikainen[4]

[1]Purdue University, West Lafayette, IN, USA.

[2]Purdue Climate Change Research Center, West Lafayette, IN, USA.

[3]Pacific Northwest National Laboratory, Richland, WA, USA.

[4]University of Eastern Finland, Kuopio, Finland.

[5]University of Helsinki, Helsinki, Finland.

[6]Finnish Environment Institute, Helsinki, Finland.

Contents of this file

Figures S1 to S3 Tables S1 to S3

Introduction

The water nutrient concentration map is interpolated using the nearest-neighborhood approach at 1°×1° resolution. Therefore, there are data values over the ocean but will not be actually used in the simulations.

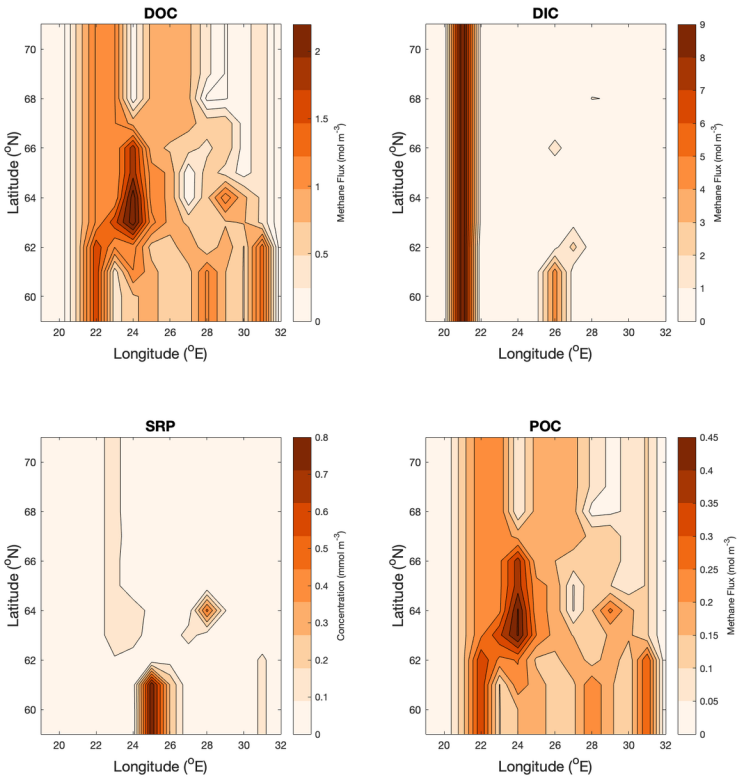

Figure S1. Interpolated water nutrient concentrations.

Posted on 22 Nov 2022 — CC-BY-NC-ND 4 — https://doi.org/10.1002/essoar.10501637.1 — This a preprint and has not been peer reviewed. Data may be preliminary.

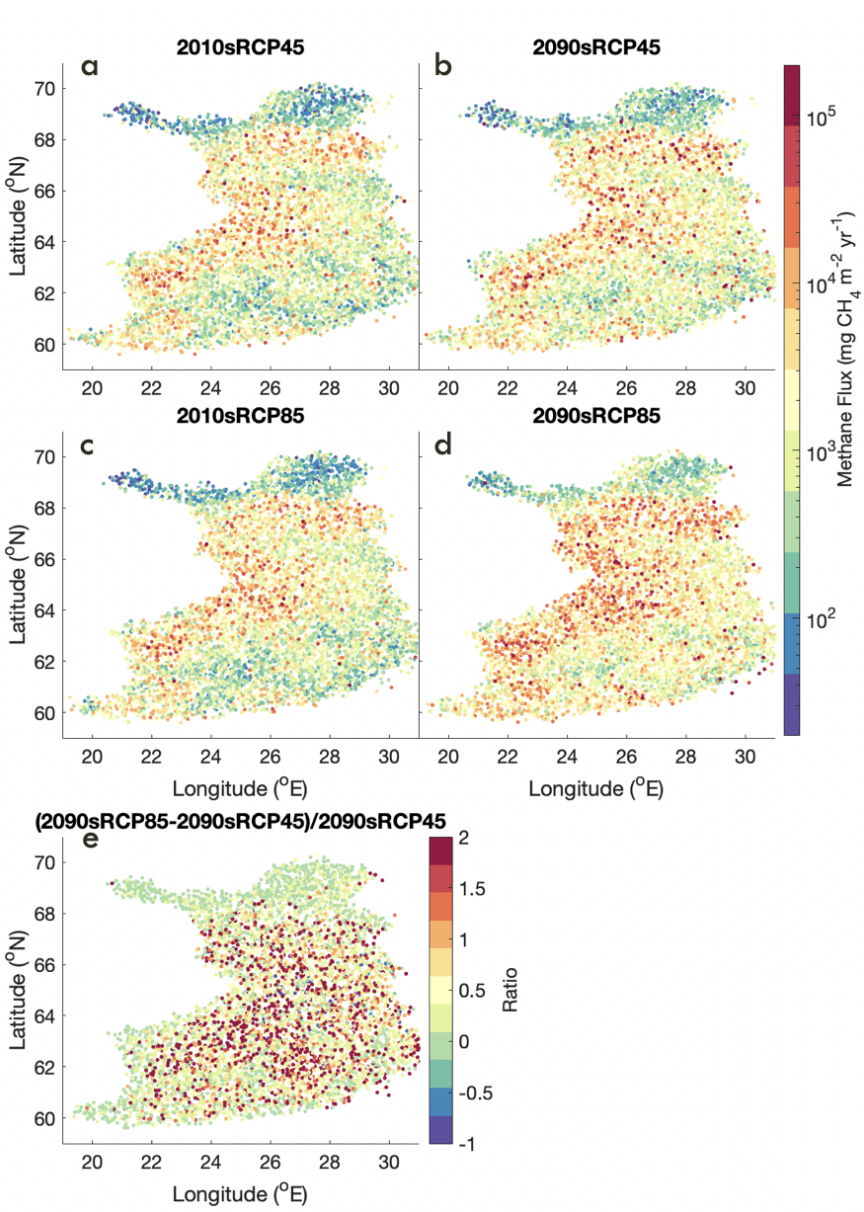

Figure S2. CH4 flux maps (a)˜(d) and percentage difference between RCP8.5 and RCP4.5 in the 2090s (e).

Figure S3. Mean annual air temperature.

Table S1. Parameter definitions and value ranges.

Table S2. Mean annual full-profile water temperature.

Posted on 22 Nov 2022 — CC-BY-NC-ND 4 — https://doi.org/10.1002/essoar.10501637.1 — This a preprint and has not been peer reviewed. Data may be preliminary.

		2010s	2090s	Increase (%)
RCP4.5	North	4.9	5.6	14.2
	South	6.8	7.7	12.9
	All	6.4	7.2	13.1
RCP8.5	North	4.9	6.5	33.5
	South	6.8	8.8	28.5
	All	6.4	8.3	29.5

Table S3. Annual ice-on days.

		2010s	2090s	Decrease (%)
RCP4.5	North	208.2	185.7	10.8
	South	171.6	149.0	13.2
	All	174.2	152.3	12.6
RCP8.5	North	207.8	159.0	23.5
	South	164.1	108.2	34.1
	All	167.3	112.4	32.8

Posted on 22 Nov 2022 — CC-BY-NC-ND 4 — https://doi.org/10.1002/essoar.10501637.1 — This a preprint and has not been peer reviewed. Data may be preliminary.

Rising methane emissions from Finnish lakes due to climate warming and increasing ice-free days

Mingyang Guo[1], Qianlai Zhuang[1,2], Zeli Tan[3], Narasinha Shurpali[4], Sari Juutinen[5], Pirkko Kortelainen[6], Pertti J. Martikainen[4]

[1]Purdue University, West Lafayette, IN, USA.

[2]Purdue Climate Change Research Center, West Lafayette, IN, USA.

[3]Pacific Northwest National Laboratory, Richland, WA, USA.

[4]University of Eastern Finland, Kuopio, Finland.

[5]University of Helsinki, Helsinki, Finland.

[6]Finnish Environment Institute, Helsinki, Finland.

Corresponding author: Qianlai Zhuang (qzhuang@purdue.edu)

Key Points:

- Finnish lake methane emissions are increasing from current 0.12±0.03 Tg yr^{-1} to future 0.20±0.05 Tg yr^{-1}
- Lake water and sediment temperature warming leads to higher methane production rates
- Longer ice-free days lead to longer emission periods and larger annual emissions

Abstract

Lakes account for about 10% of the boreal landscape and are responsible for approximately 30% of biogenic methane emissions. However, its quantification is still of large uncertainty under changing climate conditions. Finland has the densest lake system in the world with most lakes situated in the boreal zone. This study uses a large observational dataset of lake methane concentrations to constrain its methane emissions with an extant process-based lake biogeochemical model. We found that the total current diffusive emission from Finnish lakes is 0.12±0.03 Tg CH_4 yr^{-1} and will increase by 26-59% by the end of this century. We discovered that while warming lake water and sediment temperature played an important role, the climate impact on ice-on periods was a key indicator to the degree of emission increase in the future. We concluded that these boreal lakes remain as a significant methane source under warming climate in this century.

Plain Language Summary

Lakes are an important component of the boreal landscape. They are responsible for a large amount of biogenic methane emissions in the Arctic region. However, the quantification is still of large uncertainty under a changing climate. Finland has the densest lake system in the world with most lakes situated in the boreal zone. This study simulates the Finnish lake methane emissions using an extant process-based lake biogeochemistry model. The model was constrained by a large observational dataset of lake methane concentrations. We found that the total current diffusive emission from Finnish lakes is 0.12±0.03 Tg CH_4 yr^{-1} and will increase by 26-59% by the end of this century. We discovered that while warming lake water and sediment temperature contributed to the increase of methane emissions, the shortening ice-on period was the key indicator to the growth degree in the future. We concluded that these boreal lakes remain as a significant methane source under warming climate in this century.

1 Introduction

Atmospheric methane (CH_4) is the second major greenhouse gas after carbon dioxide. Although it only contributes to about 20% of the warming effect, its global warming potential is 28 times higher than carbon dioxide (Lashof et al., 1990; Myhre et al., 2013; IPCC, 2014) Over the past two decades, freshwater including lakes, reservoirs, streams and rivers are receiving an accumulating attention as important global methane sources (Bastviken et al., 2011; Prairie et al., 2013; Saunois et al., 2016). However, studies have shown large uncertainties in the estimation of freshwater methane emissions (Kirschke et al., 2013). A better estimation of the present and future lake methane emissions would largely benefit from critical improvement in watercourse mapping and CH_4 flux measurements (Saarnio et al., 2008; Kirschke et al., 2013).

Finland has one of the densest inland water systems in the world with over 200,000 water bodies over the whole country. Nearly all the lakes are in the boreal region. Ranta10 is a topologically corrected spatial dataset maintained by Finnish Environment Institute (SYKE). It contains geographical coordinate and area information of 214,995 lakes, covering 37,595 km^2 of the land surface. It is higher in spatial resolution than the Global Lakes and Wetlands Database Level 3 (GLWD-3) which only comprises 4509 lakes, reservoirs and rivers covering around 8,000 km^2 in Finland. The Ranta10 database offers a unique opportunity for modeling exercises since the smaller lakes are found to have higher methane fluxes per unit area (Juutinen et al., 2009; Holgerson et al., 2016; Sasaki et al., 2016) and are more sensitive to climate change

(Sanches et al., 2019). Additionally, Juutinen et al., (2009) have provided the measured water temperature, nutrients and methane concentrations in 207 Finnish lakes.

By using these datasets, our aim is to (1) evaluate methane emissions from the boreal lakes in Finland under climate change during three decadal periods spanning from 1990 to the end of this century using a process-based lake biogeochemical model (Tan et al., 2015a and 2017); (2) understand the driving factors of lake methane emission changes and (3) discuss the implication on the whole Arctic lake emissions.

2 Materials and Methods

2.1 Model configuration

The Arctic Lake Biogeochemistry Model (ALBM) is a one-dimensional process-based lake biogeochemical model designed for predicting both thermal and carbon dynamics of aquatic ecosystems. It mainly consists of several modules including those for the radiative transfer, the water/sediment thermal circulation, the water/sediment biogeochemistry, and the gas diffusive and ebullitive transportation. Detailed information about ALBM can be found in Tan et al. (2015a and 2017). We introduce the key governing equations of methane processes in ALBM below.

Methane production rate P in sediments is calculated from labile carbon content and temperature:

$$P = R_c C_{labile} PQ_{10}^{(T-T_{pr})/10} \quad (1)$$

Where R_c is the fraction of carbon converted per year, C_{labile} is the labile carbon content, PQ_{10} is the factor by which the production rate increases with a 10 °C rise in temperature, and T_{pr} is a reference temperature. Methane can be oxidized after being released into the water and the oxidation rate V_{oxid} is described by

$$V_{oxid} = Q_{CH_4} OQ_{10}^{(T-T_{or})/10} \frac{C_{O_2}}{k_{O_2} + C_{O_2}} \frac{C_{CH_4}}{k_{CH_4} + C_{CH_4}} \quad (2)$$

where Q_{CH_4} is the maximum oxidation potential, OQ_{10} is the factor by which the oxidation potential increases with a 10 °C rise in temperature, T_{or} is a reference temperature, C_{O_2} and C_{CH_4} and gas concentrations, and k_{O_2} and k_{CH_4} are the Michaelis-Menten constants. Together, the modeled methane concentration in water columns is calculated by

$$\frac{\partial C_{CH_4}}{\partial t} = \frac{\partial}{\partial z}\left(D_{CH_4} \frac{\partial C_{CH_4}}{\partial z}\right) - V_{oxid} \pm L_{CH_4} \quad (3)$$

where D_{CH_4} is the diffusivity of methane, and L_{CH_4} is the gas exchange between bubbles and the ambient water. Finally, methane within water is transported to the atmosphere. The diffusive transfer velocity *k* is defined as

$$k = 2.778 \times 10^{-6} \times (2.07 + 0.125 \times U_{10}^{1.7}) \times \left(\frac{Sc_m}{600}\right)^{0.5} \quad (4)$$

where U_{10} is the 10-m wind speed (m s^{-1}) and Sc_m is the Schmidt number of methane. Since we lacked ebullition flux observations and therefore, we were unable to validate the modeled ebullition emissions, we only quantified diffusive emissions in this study.

The numerical experiment consists of three steps: (1) the model calibration using observations of diffusive emissions during 1998-1999 from 39 individual lakes; (2) regional simulations of 1990-1999 by applying ALBM to the Ranta10 data product; (3) regional simulations of 2010-2019 and 2090-2099 under the representative concentration pathway (RCP) scenarios of RCP4.5 and RCP8.5. For all the simulations, a spin-up period of two years was run.

2.2 Data

Model forcing data include air temperature, surface pressure, 10-m wind, relative humidity, precipitation, snowfall, downward short-wave radiation and downward long-wave radiation. The historical simulation was driven by the climate data retrieved from the European Center for Medium-Range Weather Forecasts (ECMWF) Interim re-analysis (ERA-Interim) with a resolution of 0.75°×0.75°, and organized into daily datasets. For future climate scenarios, we used a down-scaled bias-corrected dataset of he Intersectoral Impact Model Intercomparison Project (ISIMIP) output from HadGEM2-ES (Frieler et al., 2017) that is set on a 0.5°×0.5° global grid and is divided into daily time steps. This climate dataset is bias-corrected based on ERA-Interim, which guarantees the consistency of historical and future simulation results.

Lakes with area smaller than 100 m^2 were omitted in our simulations due to the large uncertainties in the mapping of these lakes, leaving 210,773 lakes covering 36,690 km^2. In general, the region north of 67 °N has the highest lake density but relatively sparse observations of thermal or carbon dynamics (Figure 1a, 1b). Over 90% of the lakes are smaller than 0.1 km^2 (Figure 1c), which are not included in the GLWD-3 database. Depth information was lacking for over 90% of the lakes even by combining the Ranta10 and the GLWD-3 database. As such, we applied a statistical approach to construct the full lake depth dataset. We first grouped the lakes into 10 bins bounded by areas of 0, 0.01, 0.05, 0.1, 0.5, 1, 2, 3, 4, 5, 10, 100, 1500 km^2, respectively. We then generated a histogram of depths in each group. We randomly assigned the depths following the fitted probability distribution in each group. By following this approach, we aimed to construct

lakes profiles that match the diversity of the real lake system in Finland. In terms of lake bathymetry, we assume a linear decrease of the cross-section area with increasing depth.

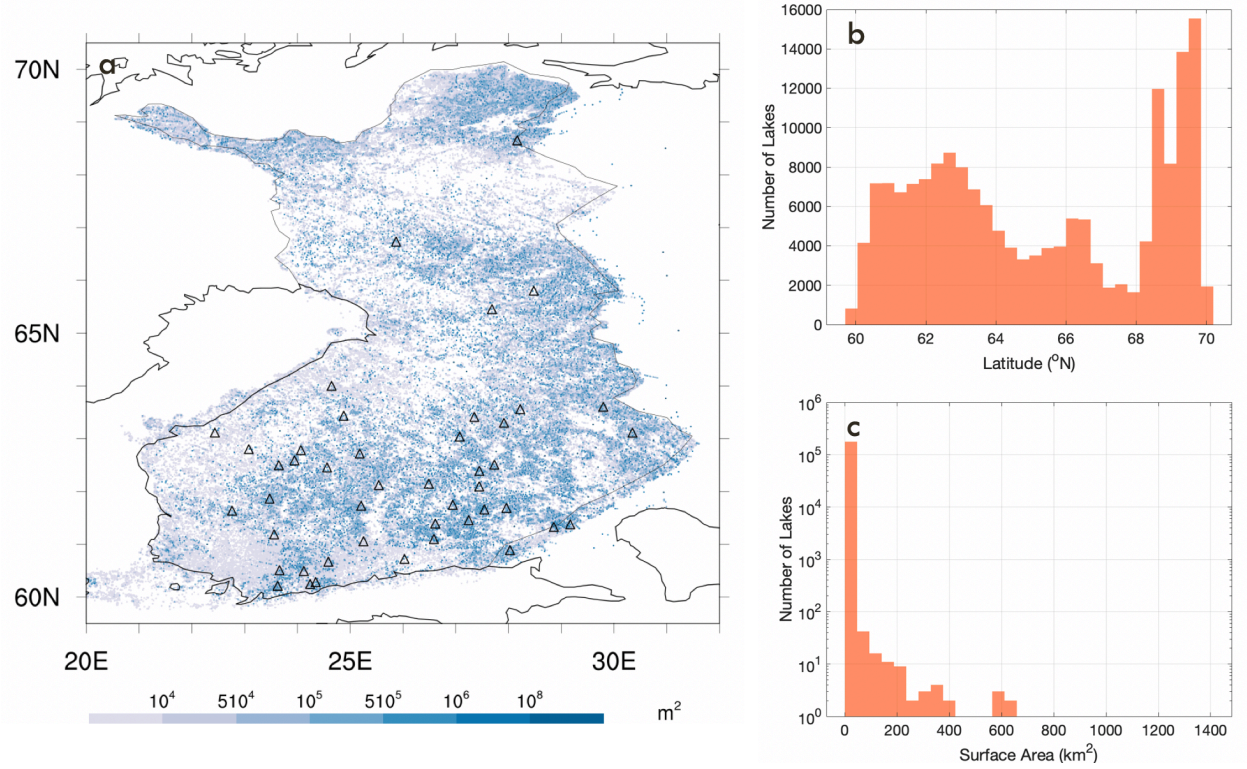

Figure 1. Map of Finland with lakes color coded by surface area (a). Triangles indicate the lakes used for calibration. Distribution of lake latitudes and surface areas, respectively (b) and (c).

The water temperature, nutrient and methane concentrations were measured at four levels of depth four times in either year 1998 or 1999. The methane diffusive fluxes were calculated following Eq.4. Technical details were introduced in Juutinel et al. (2009). For the simulation purpose, several assumptions and approximations were made on for carbon and phosphorous input that are required by the model, including 1) dissolved organic carbon (DOC) concentration is equal to total organic carbon (Mopper et al., 2006); 2) dissolved inorganic carbon (DIC) concentration is calculated from pH and alkalinity; 3) soluble reactive phosphorus (SRP) concentration is equal to PO_4 and 4) particular organic carbon (POC) concentration is approximately 1/5.1 of DOC concentration (Rachold et al., 2014). We produced an input map of DOC, DIC, PO_4 and SRP at 1°×1° with observations averaged at each grid and filled with nearest-neighbor interpolation (Figure S1).

2.3 Model calibration

Since the lake shape has large impacts on the thermal dynamics (Mazumder et al., 1994; Woolway et al., 2016 and 2017) and carbon dynamics (Schilder et al., 2013; Pighini et al., 2018), we decided to conduct calibration and thus simulations by lake groups. The simulated lakes were firstly divided by the surface area into six groups

bounded by 0.05, 0.1, 0.2, 1, 10, 1000 km^2, respectively and then by the shape factor, defined by $\sqrt{\text{Area}}/\text{Depth}$, into two groups bounded by 0.1 and 10, respectively. Thirty-nine lakes that represent various depths and shape factors were selected from the observations and used for calibration.

We calibrated the model based on the water temperature (eight parameters) and the methane diffusive emission (seven parameters). The descriptions and corresponding ranges of the parameters are listed in Table S1. Since, the sensitive parameters of the water temperature and the methane diffusive emission simulations were different, the calibration was conducted separately. We first applied a Monte Carlo calibration method for water temperature calibration using 6000 sets of parameters for each lake. For the methane emissions, a 'history matching' method (Mcneall et al., 2013; Williamson et al., 2013, 2015 and 2017}) was adopted for higher accuracy and efficiency. This method requires less computation time than a full Monte Carlo simulation (Williamson et al., 2013) and has been shown to largely reduce simulation biases (Salter et al., 2018). It was carried out in the following steps: 1) use the Sobol sequence sampling method (Sobol, 1967) to generate a perturbed parameter ensemble (PPE) by sampling from the parameter space; 2) run simulations for all perturbed parameter (PP) sets; 3) rule out regions of the parameter space based on the outputs where a predefined metric exceeds the threshold; 4) repeat step 1 to 3 until a certain number of iterations or the desired outcome is achieved. In our study, 1200 PP sets were generated for each round and the metric used was the root-mean-square error (RMSE) defined by

$$RMSE = \sqrt{\frac{\sum_{i=1}^{N}(O_{Flux} - S_{Flux})^2}{N}} \quad (5)$$

where O_{Flux} is the observed annual methane flux, S_{Flux} is the simulated, and N is the number of observation sites. Parameter spaces resulting in RMSEs over the 50% of the observations at each site were ruled out at each round, until 3 rounds were finished.

2.4 Sensitivity and uncertainty analysis

For parametric sensitivity analysis, running the model for the whole region over a 10-year time period takes about five days, and thus it would be rather time-consuming to run full PPE simulations. Instead, we run short PPE simulations for a single year from 1998 to 1999 with 20 PP sets sampled from the remaining parameter space after history matching. It has been proved that the results from short simulations match well to the longer-term simulations (Qian et al., 2016), especially when methane emission response

to air temperature is a relatively well-defined process (Sanches et al., 2019) and thus can be captured within a one-year range.

3 Results and discussions

3.1 Model performance

The model overall showed good performances on reproducing both water temperature and methane emissions (Figure 2) with an average RMSE of 1.59 °C for full-profile water temperature simulations and a correlation coefficient (r) of 0.69 for methane emissions. There was a point with the observation showing over 200 mmol m^{-2} yr^{-1} while the corresponding modeled value was only one third of the observed value. This underestimation was possibly due to the missing of DOC concentration measurement at this lake. Since it is a very humic shallow lake (color > 90 Pt mg L^{-1}, mean depth < 3m, see Juutinen et al., 2009), taking the average value of other lakes in the same grid likely results in a much lower DOC concentration.

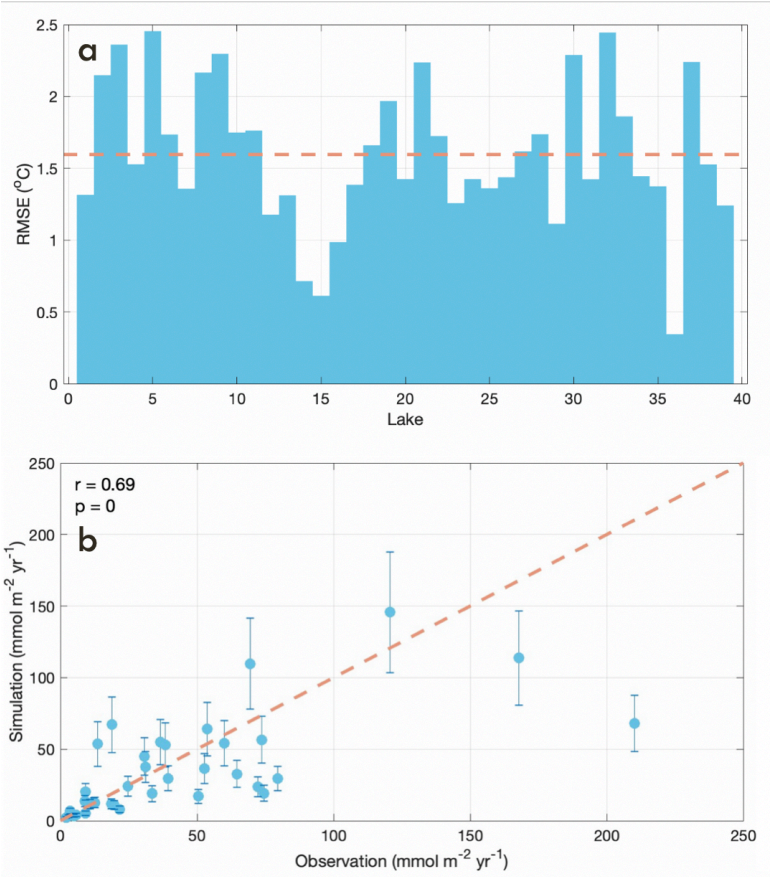

Figure 2. Water temperature simulation RMSEs with the mean (dashed line, a). Observed vs. simulated annual methane diffusive emissions (b).

Note that the uncertainty range can be wider using the history matching approach than using the Bayesian method, which is expected because the former focuses on

confining the output whereas the latter on confining the input, i.e. the parameters themselves. Therefore, the PPE by the latter would be more representative of the parameter distributions and thus results in smaller uncertainties.

3.2 Annual methane emission estimation

Simulations indicated that the methane emissions from Finnish lakes were 0.12±0.03 Tg CH_4 yr^{-1} in the 1990s. There was only 4% and 6% increase during period 1990~2019 under RCP4.5 and RCP8.5, respectively (Figure 3) when less than 2 °C of warming has occurred. Walter et al. (2007) estimated that the current total diffusion from all lakes north of 45 °N is 1.12±0.22 Tg CH_4 yr^{-1}. If assuming the same total lake area over the Arctic and the same lake size distribution as the Finnish lakes, we estimated the emission to be 3.65±1.06 Tg CH_4 yr^{-1}. The difference can be due to: 1) Walter et al. (2007) simply used a constant flux calculated from several glacial lakes and thermokarst lakes for all other lakes, which may underrepresent the variation; 2) Based on several Siberian thaw lakes, an ice-free period of 120 days was assumed in the calculation for all lakes, leading to underestimation in warmer regions, for example, the mean ice-off periods in Finland is about 170 days. Another reason that their estimation may be conservative is the assumption that the total lake area in the GLWD is underestimated by 50%, whereas our mapping indicates that the actual underestimation is 78% in the boreal region. If accounting for this mapping bias, we estimated the diffusive emission to be 8.38±2.43 Tg CH_4 yr^{-1} from all lakes north of 45 °N.

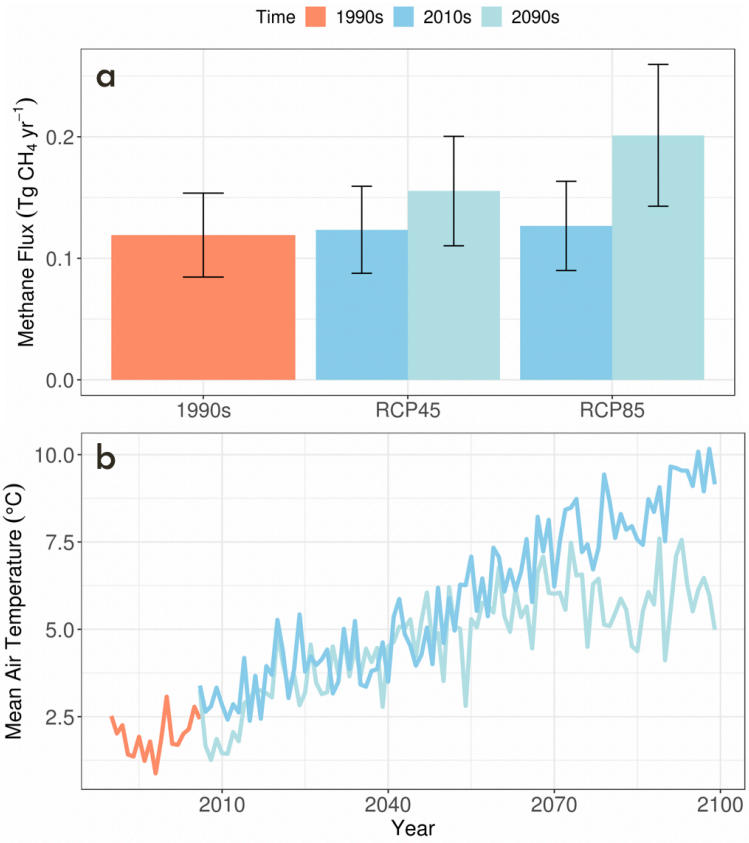

Figure 3. Simulated diffusive CH_4 emissions (a) and mean annual air temperature (b).

We estimated that the Finnish lake diffusive methane emissions will increase by 25.8% from 0.12±0.04 to 0.16±0.05 Tg CH_4 yr^{-1} under the RCP4.5 scenario while they will increase by about 58.9% from 0.13±0.04 to 0.20±0.06 Tg CH_4 yr^{-1} under the RCP8.5. The magnitude of the growth is relatively small compared to Tan et al. (2015a and 2015b) who predicted an 80% increase in the Northern Europe even under the RCP2.6 scenario. It is likely because we didn't model ebullition emission. It has been found that future warming may have much larger effects on ebullition even altering diffusive-emission dominant lakes to ebullition-dominant ones (Aben et al., 2017). Therefore, the amount of extra increase is likely due to the enhanced ebullition processes.

Based on the analysis of 297 lakes worldwide, Sanches et al., (2019) found that considering only diffusive emissions would cause an average underestimation of 277%. By taking into account also the ebullition emissions, the current annual methane emission for all northern lakes would be 31.59±9.16 Tg CH_4 yr^{-1}, in the upper range of the previous estimation, 24.2±10.5 Tg CH_4 yr^{-1} by Water et al. (2007). Furthermore, Aben et al. (2017) predicted that ebullition would increase faster than diffusive emissions, by 51% with 4 °C warming. Similarly, Thornton et al. (2015) predicted an increase of around 56% from the present to the 2040-2079 period using observations from three subarctic lakes in Sweden. If, based on the warming magnitude, we estimate a 50% and 100% growth of ebullition emissions under the RCP4.5 and RCP8.5, respectively, this will give a total methane emission of 43.2±12.5 Tg CH_4 yr^{-1} and 56.65±16.43 Tg CH_4 yr^{-1}, respectively from the whole Arctic lakes. This projection is about 70% higher than the previous 32.7±5.2 Tg CH_4 yr^{-1} by Tan et al. (2015b), which can be expected because they used the GLWD-3 map for lakes north of 60 °N.

3.3 Spatial features of methane emissions and causes

Apart from the temporal trend, we also looked into the spatial features. Methane emission hotspots generally match with the areas that are dense with small lakes (Figure1a, Figure S2a-d). This was also found in previous studies (Bastviken et al., 2004; Del Sontro et al., 2016; Saarnio et al., 2008; Wik et al., 2013). This spatial variability be explained by: 1) methane can be oxidized along the of diffusive transportation, and thus deeper lakes usually mean more loss by oxidation and 2) it was found that smaller lakes are more likely to have abundant organic substrates in their sediments, and thus they are potentially more productive for methane.

We also found differences between the southern and the northern part of Finland. Firstly, the south has larger methane emissions under all the scenarios, which is intuitive because it’s warmer. However, the south also experiences more severe increase of emissions than the north (Figure S2e). Some lakes in the south can increase by 200% in their emissions while the increase in the north is much less severe. Here we define the south and north by

manually drawing a line at latitude 67.5 °N, which also happens to be the latitude that divides Finland into air temperature above and below 0 °C in the 2010s.

We suspected that this difference in the degree of emission increase was caused by the fact that the south warming faster than the north. However, it turned out that both parts are warming by about the same 4 °C by the end of this century (Figure S2), and the water temperature in the north is even warming a little bit faster than the south (Table S2). Therefore, the absolute increase of air temperature itself cannot explain the difference. Instead, we found that it is actually the ice condition that makes a difference. By the same degree of warming, the mean ice-on days in the north decrease much slower than the south (Table S3). Methane fluxes can be blocked by ice covers and then oxidized in the water columns during ice-on seasons. Therefore, a large amount of methane trapped by ice covers presently could be emitted into the atmosphere in the future. Generally, ice covers of lakes in the north are thicker and thus would take higher warming to melt before methane can be released in winter.

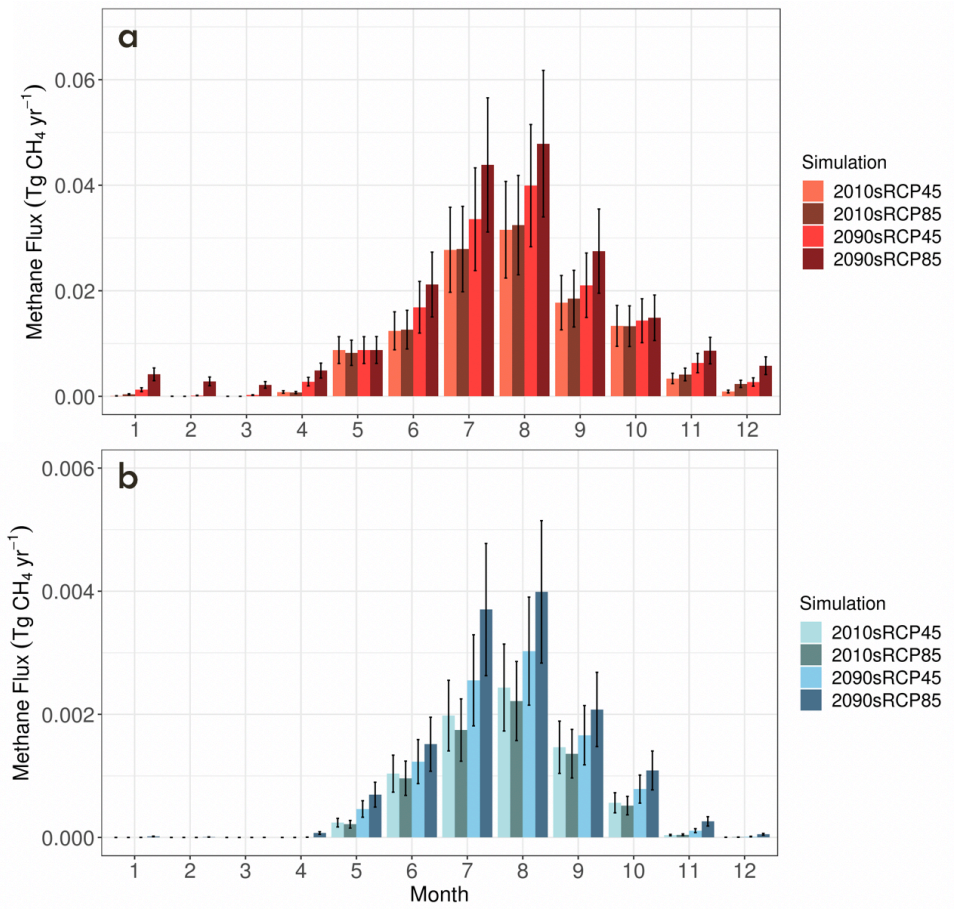

Figure 4. (a) and (b) CH_4 emissions by month from lakes south of and north of 67.5 °N, respectively. Note different scales on y-axis.

The influence of ice-on days is also reflected in the seasonality of lake methane emissions (Figure 4). If we only look at the ice-off seasons, it's all the same pattern in both regions, that higher emission during warmer months under warmer scenarios. However, it's really the ice-on season that explains the difference. From December to April, we hardly see any emission in the 1990s, but we expect much higher emissions in the future for the period due to warming. Such shift may not be initiated in the north within this century and therefore, the increase of lake methane emissions in the north is much less severe.

3.4 Uncertainty quantification

Our model simulations did not consider the impacts of DOC dynamics on the lake emissions. In boreal regions, in addition to the climate change, many boreal lakes have been found to be experiencing moderate to severe browning over the last decades, probably due to the increased import of DOC from soils (Haaland et al., 2010; Isidorova et al., 2016; Monteith et al., 2007; Roulet et al., 2006; Seekell et al., 2015). If DOC concentrations increase at the current rate, they can be twice high by the end of this century (de Wit et al., 2016). It's found that the methane diffusive emission is positively related to DOC concentrations (Sanches et al., 2019). However, the relationship can involve several processes. More nutrients will be available for microbes and primary producers. However, the turbidity will weaken photosynthesis that causes methane oxidation. The model will need to be improved to predict the effect of lake browning. So far, no study has included this effect when estimating future methane emissions.

We assumed a constant landscape in our simulations that no lake expansion or drainage was considered until 2100. This is because boreal lakes in Finland are not formed over permafrost and thus not affected by the active response of thawing and ground water penetration processes in responding to climate as thermokarst lakes. Wik et al., (2016) predicted that with 20-day increase of ice periods, even the total lake area decreases by 30%, the total methane emission can still grow by 20% which is 10% less than assuming constant lake area. Therefore, we will still expect the boreal lake methane emissions will be affected by considering the lake area changes. Incorporating lake areal dynamics into future quantification is necessary.

5 Conclusions

Lakes are an important component of arctic and subarctic landscape. Our process-based lake biogeochemistry model simulation reveals that diffusive methane emissions from boreal lakes in Finland amount to 0.12±0.03 Tg CH_4 yr^{-1} during the 1990s and will increase by 25.8% to 58.9% by the end of the 21st century depending on the warming scenario. The driving factors are two-fold. We found that higher air temperature will lead to higher lake water temperature and thus more active methanogenesis. Warming also results in shorter ice-on periods, leading to longer emission days. The ice-free days are a more dominant factor than the lake temperature change impacts. If extrapolating the ratio of diffusion to ebullition emissions to the region, we

estimated the annual regional lake emissions are 31.59±9.16 Tg CH_4 yr^{-1} at the present and 30.7-73.08 Tg CH_4 yr^{-1} during the last decade of this century from all lakes north of 45 °N.

Acknowledgments and Data

This study is supported through a projected funded to Q.Z. by NASA (NNX17AK20G) and a project from the United States Geological Survey (G17AC00276). The supercomputing is provided by the Rosen Center for Advanced Computing at Purdue University. The Ranta10 dataset is available at https://www.syke.fi/en-US/Open_information/Spatial_datasets/Downloadable_spatial_dataset#R.

References

Aben, R. C. H. , Barros, N. , Van Donk, E. , Frenken, T. , Hilt, S. , & Kazanjian, G. , et al. (2017). Cross continental increase in methane ebullition under climate change. *Nature Communications, 8*(1), 1682. doi: 10.1038/s41467-017-01535-y

Asit, Mazumder, William, & Taylor, D. . (1994). Thermal structure of lakes varying in size and water clarity. *Limnology and Oceanography*. doi:10.4319/lo.1994.39.4.0968

Bastviken, D. , Tranvik, L. J. , Downing, J. A. , Crill, P. M. , & Enrich-Prast, A. . (2011). Freshwater methane emissions offset the continental carbon sink. *Science, 331*(6013), 50-50. doi:10.1126/science.1196808

Cael, B. B. , & Seekell, D. A. . (2016). The size-distribution of earth's lakes. *Scientific Reports, 6*, 29633. doi: 10.1038/srep29633

Core Writing Team. (2014). Climate change 2014: synthesis report. *Contribution of working groups I, II and III to the fifth assessment report of the intergovernmental panel on climate change*, 151.

Del Sontro, T. , Boutet, L. , St-Pierre, A. , Del Giorgio, P. A. , & Prairie, Y. T. . (2016). Methane ebullition and diffusion from northern ponds and lakes regulated by the interaction between temperature and system productivity. *Limnology and Oceanography*. doi:10.1002/lno.10335

Doug, M. N. , Jonny, W. , Ben, B. , Richard, B. , Peter, C. , & Andy, W. , et al. (2016). The impact of structural error on parameter constraint in a climate model. *Earth System Dynamics Discussions*, 1-37. doi:10.5194/esd-2016-17

Haaland, S. , Hongve, D. , Laudon, H. , Riise, G. , & Vogt, R. D. . (2010). Quantifying the drivers of the increasing colored organic matter in boreal surface waters. *Environmental Science & Technology, 44*(8), 2975-2980. doi: 10.1021/es903179j

Holgerson, M. A. , & Raymond, P. A. . (2016). Large contribution to inland water co2 and ch4 emissions from very small ponds. *Nature Geoscience*. doi:10.1038/ngeo2654

van Huissteden, J. , Berrittella, C. , Parmentier, F. J. W. , Mi, Y. , Maximov, T. C. , & Dolman, A. J. . (2011). Methane emissions from permafrost thaw lakes limited by lake drainage. *Nature Climate Change, 1*(2), 119-123. doi: 10.1038/nclimate1101

Juutinen, S. , Rantakari, M. , Kortelainen, P. , Huttunen, J. T. , Larmola, T. , & Alm, J. , et al. (2009). Methane dynamics in different boreal lake types. *Biogeosciences, 6*(2), 209-223. doi:10.5194/bg-6-209-2009

Isidorova, A., Bravo, A. G., Riise, G., Bouchet, S., Bjorn, E. and Sobek, S. (2016). The effect of lake browning and respiration mode on the burial and fate of carbon and mercury in the sediment of two boreal lakes. *Journal of Geophysical Research: Biogeosciences, 121*(1), 233-245. doi: 10.1002/2015jg003086

Jennifer, Joyce, Paul, W., and Jewell. (2003). Physical controls on methane ebullition from reservoirs and lakes. *Environmental & Engineering Geoscience*. doi:10.2113/9.2.167

Katey, W. A. , Thomas, S. V. D. , Ingmar, N. , Steve, F. , Abraham, E. , & Ronald, D. , et al. (2018). 21st-century modeled permafrost carbon emissions accelerated by abrupt thaw beneath lakes. *Nature Communications, 9*(1), 3262-. doi: 10.1038/s41467-018-05738-9

Kirschke, S. , Bousquet, P. , Ciais, P. , Saunois, M. , & Zeng, G. . (2013). Three decades of global methane sources and sinks. *Nature Geoscience, 6*(10), 813-823. doi: 10.1038/ngeo1955

Larsen, S. , Andersen, T. , & Hessen, D. O. . (2011). Climate change predicted to cause severe increase of organic carbon in lakes. *Global Change Biology, 17*(2), 1186-1192. doi: 10.1111/j.1365-2486.2010.02257.x

Lashof, D. A. , & Ahuja, D. R. . (1990). Relative contributions of greenhouse gas emissions to global warming. *Nature, 344*(6266), 529-531. doi:10.1038/344529a0

Mazumder, A., & Taylor, W. D. (1994). Thermal structure of lakes varying in size and water clarity. *Limnology and Oceanography*, *39*(4), 968-976. doi: 10.4319/lo.1994.39.4.0968

Mcneall, D. J. , Challenor, P. G. , Gattiker, J. R. , & Stone, E. J. . (2013). The potential of an observational data set for calibration of a computationally expensive computer model. *Geoscientific Model Development, 6*(5), 1715-1728. doi:10.5194/gmd-6-1715-2013

Monteith, D., Stoddard, J., Evans, C. *et al.* (2007). Dissolved organic carbon trends resulting from changes in atmospheric deposition chemistry. *Nature* **450,** 537–540. doi:10.1038/nature06316

Mopper, K. , & Qian, J. . (2006). *Water Analysis: Organic Carbon Determinations*. *Encyclopedia of Analytical Chemistry*. John Wiley & Sons, Ltd. doi:10.1002/9780470027318.a0884

Myhre, G., D. Shindell, F.-M. Bréon, W. Collins, J. Fuglestvedt, J. Huang, D. Koch, J.-F. Lamarque, D. Lee, B. Mendoza, T. Nakajima, A. Robock, G.Stephens, T. Takemura and H. Zhang, 2013: Anthropogenic and Natural Radiative Forcing. In: Climate Change 2013: The Physical Science Basis. Contribution of Working Group I to the Fifth Assessment Report of the Intergovernmental Panel on Climate Change [Stocker, T.F., D. Qin, G.-K. Plattner, M. Tignor, S.K. Allen, J. Boschung, A. Nauels, Y. Xia, V. Bex and P.M. Midgley (eds.)]. Cambridge University Press, Cambridge, United Kingdom and New York, NY, USA, pp. 659–740. doi:10.1017/ CBO9781107415324.018.

Paltan, H. , Dash, J. , & Edwards, M. . (2015). *A refined mapping of Arctic lakes using Landsat imagery*. Taylor & Francis, Inc. doi: 10.1080/01431161.2015.1110263

Pighini, S., Ventura, M., Miglietta, F., & Wohlfahrt, G. (2018). Dissolved greenhouse gas concentrations in 40 lakes in the Alpine area. *Aquatic sciences*, *80*(3), 32. doi: 10.1007/s00027-018-0583-2

Prairie, Y. , & Del Giorgio, P. . (2013). A new pathway of freshwater methane emissions and the putative importance of microbubbles. *Inland Waters, 3*(3), 311-320. doi:10.5268/IW-3.3.542

Qian, Yun, Jackson, Charles, Giorgi, & Filippo, et al. (2016). Uncertainty quantification in climate modeling and projection. *Bulletin of the American Meteorological Society, 97*(5), 160106131713003. doi:10.1175/BAMS-D-15-00297.1

Rachold, V., Eicken, H., Gordeev, V. V., Grigoriev, M. N., Hubberten, H.-W., Lisitzin, A. P., et al. (2014). Modern Terrigenous Organic Carbon Input to the Arctic Ocean. In The organic carbon cycle in the arctic ocean (pp. 33-55). doi:10.1007/978-3-642-18912-8_2

Roulet, N. , & Moore, T. R. . (2006). Environmental chemistry: browning the waters. *NATURE, 444*(7117), 283-284. doi:10.1038/444283a

Saarnio, S. , Winiwarter, W. , & Leit?O, J. . (2009). Methane release from wetlands and watercourses in europe. *Atmospheric Environment, 43*(7), 1421-1429. doi: 10.1016/j.atmosenv.2008.04.007

Salter, J. M., Williamson, D. B., Scinocca, J., & Kharin, V. (2019). Uncertainty quantification for computer models with spatial output using calibration-optimal bases. *Journal of the American Statistical Association*, 1-24. doi: 10.1080/01621459.2018.1514306

Sanches, Lúcia Fernandes, Guenet, B. , Marinho, C. C. , Barros, N. , & Francisco, D. A. E. . (2019). Global regulation of methane emission from natural lakes. *Scientific Reports, 9*(1). doi:10.1038/s41598-018-36519-5

Sasaki, M. , Kim, Y. W. , Uchida, M. , & Utsumi, M. . (2016). Diffusive summer methane flux from lakes to the atmosphere in the alaskan arctic zone. *Polar Science*, S187396521630055X. doi:10.1016/j.polar.2016.06.010

Saunois, M. , Bousquet, P. , Poulter, B. , Peregon, A. , & Zhu, Q. . (2016). The global methane budget: 2000–2012. doi:10.5194/essd-2016-25

Schilder, J. , Bastviken, D. , Van Hardenbroek, M. , Kankaala, P. , Rinta, P. , & St?Tter, T. , et al. (2013). Spatial heterogeneity and lake morphology affect diffusive greenhouse gas emission estimates of lakes. *Geophysical Research Letters, 40*(21), 5752-5756. doi:10.1002/2013GL057669

Seekell, D.A., Lapierre, J.-F., Ask, J., Bergstrom, A.-K., Deininger, A., Rodriguez, P., and Karlsson, J. (2015). The influence of dissolved organic carbon on primary production in northern lakes. *Limnology and Oceanography, 60*(4), 1276-1285. doi: 10.1002/lno.10096

Sobol′, I. M. . (1967). On the distribution of points in a cube and the approximate evaluation of integrals. *USSR Computational Mathematics and Mathematical Physics, 7*(4), 86-112. doi:10.1016/0041-5553(67)90144-9

Sylvie, P. , Maurizio, V. , Franco, M. , & Georg, W. . (2018). Dissolved greenhouse gas concentrations in 40 lakes in the alpine area. *Aquatic Sciences, 80*(3), 32-. doi:10.1007/s00027-018-0583-2

Tan, Zeli & Zhuang, Qianlai & Walter Anthony, Katey. (2015a). Modeling methane emissions from arctic lakes: Model development and site-level study. Journal of Advances in Modeling Earth Systems. 7(2). 459-483. doi: 10.1002/2014MS000344.

Tan, Z. , & Zhuang, Q. . (2015b). Methane emissions from pan-arctic lakes during the 21st century: an analysis with process-based models of lake evolution and biogeochemistry. *Journal of Geophysical Research: Biogeosciences, 120*(12), 2641-2653. doi: 10.1002/2015JG003184

Tan Z., Q. Zhuang, N. Shurpali, M. Marushchak, C. Biasi, W. Eugster, and K. Walter Anthony. (2017). "Modeling CO2 emissions from Arctic lakes: Model development and site-level study." *Journal of Advances in Modeling Earth Systems* 9, no. 5:2190-2213. PNNL-SA-129018. doi: 10.1002/2017MS001028

Thornton, B. F., Wik, M., & Crill, P. M. (2015). Climate-forced changes in available energy and methane bubbling from subarctic lakes. *Geophysical Research Letters*, *42*(6), 1936-1942. doi: 10.1002/2015GL063189

456 Walter, K. M., Smith, L. C., & Stuart Chapin, F. . (2007). Methane bubbling from northern lakes:
457 present and future contributions to the global methane budget. *Philosophical Transactions of the*
458 *Royal Society A: Mathematical, Physical and Engineering Sciences,365*(1856), 1657-1676. doi:
459 10.1098/rsta.2007.2036

460 Wik, M. , Varner, R. K. , Anthony, K. W. , Macintyre, S. , & Bastviken, D. . (2016). Climate-
461 sensitive northern lakes and ponds are critical components of methane release. *Nature*
462 *Geoscience*. doi: 10.1038/ngeo2578

463 Williamson, D., Goldstein, M., Allison, L., Blaker, A., Challenor, P., Jackson, L., and Yamazaki,
464 K. (2013) History Matching for Exploring and Reducing Climate Model Parameter Space Using
465 Observations and a Large Perturbed Physics Ensemble. *Climate Dynamics,* 41(7), 1703-1729.
466 Williamson, D. , Blaker, A. T. , Hampton, C. , & Salter, J. . (2015). Identifying and removing
467 structural biases in climate models with history matching. *Climate Dynamics, 45*(5-6), 1299-
468 1324. doi:10.1007/s00382-014-2378-z
469 Williamson, D. , Blaker, A. T. , & Sinha, B. . (2016). Tuning without over-tuning: parametric
470 uncertainty quantification for the nemo ocean model. *Geoscientific Model Development*
471 *Discussions*, 1-41. doi:10.5194/gmd-2016-185

472 de Wit, H. A., Valinia, S., Weyhenmeyer, G. A., Futter, M. N., Kortelainen, P., Austnes, K., et
473 al. (2016). Current Browning of Surface Water will be Further Promoted by Wetter Climate.
474 *Environmental Science & Technology Letters,* 3(12), 430-435. doi: 10.1021/acs.estlett.6b00396
475 Woolway, R. I., Jones, I.D., Maberly, S. C., French, J. R., Livingstone, D. M., Monteith, D. T. et
476 al. (2016). Diel Surface Temperature Range Scales with Lake Size. PLoS ONE. 11(3),
477 e0152466. doi: 10.1371/journal.pone.0152466
478 Woolway, R. I. , & Merchant, C. J. . (2017). Amplified surface temperature response of cold,
479 deep lakes to inter-annual air temperature variability. *Scientific Reports, 7*(1), 4130.
480 doi:10.1038/s41598-017-04058-0